

Mono-Higgs signature in a singlet fermionic dark matter model

Yeong Gyun Kim*

Department of Science Education, Gwangju National University of Education, Gwangju 61204, Korea

Kang Young Lee†

Department of Physics Education & RINS, Gyeongsang National University, Jinju 52828, Korea

Soo-hyeon Nam‡

Department of Physics, Korea University, Seoul 02841, Korea

(Dated: June 26, 2025)

We investigate the production of dark matter in association with a Higgs boson at the LHC within the singlet fermionic dark matter model. We focus on final states featuring a Higgs boson accompanied by large missing transverse momentum (E_T^{miss}), where the Higgs decays into a $b\bar{b}$ pair in the ATLAS analysis and into a ZZ pair in the CMS analysis. Assuming light dark matter fermions with a mass of approximately 1 GeV, we find that the predicted production yields in this model are compatible with, or even exceed, those of the benchmark scenarios studied in the recent experimental analyses, particularly in the low E_T^{miss} region, under parameter sets allowed by current collider bounds and dark matter constraints. Therefore, we expect that some exclusion limits on the model parameters introduced in this work may be derived from existing ATLAS and CMS mono-Higgs search results, and that the mono-Higgs production in this model can be directly probed at the future High-Luminosity phase of the LHC.

arXiv:2506.20113v1 [hep-ph] 25 Jun 2025

* ygkim@gnue.ac.kr

† kylee.phys@gnu.ac.kr; corresponding author

‡ glvsh@gmail.com; corresponding author

I. INTRODUCTION

The existence of dark matter (DM) is strongly supported by numerous astrophysical and cosmological observations, such as galaxy rotation curves, the Bullet Cluster, gravitational lensing, and anisotropies in the cosmic microwave background (CMB) [1–5]. We now seek to understand whether DM particles interact with Standard Model (SM) particles and, if so, what signatures such interactions may produce. A massive DM particle that interacts with SM particles with a strength comparable to that of the weak interaction, known as a weakly interacting massive particle (WIMP), is one of the most popular DM candidates.

If there exist non-gravitational interactions between DM particles and the SM matter, it may be possible to search for DM at colliders. A promising collider signature of WIMPs is the production of a single visible SM particle accompanied by large missing transverse energy (E_T^{miss}). Since DM particles escape the detector without interacting, they leave behind an imbalance in the transverse momentum. Such events are largely model-independent and are characterized by a significant transverse momentum imbalance recoiling against a visible SM particle. Collider studies have focused on event topologies where a single SM particle is produced in association with DM particles, leading to so-called mono- X signatures. To date, a variety of mono- X signatures with E_T^{miss} have been explored, such as mono-jet [6–8], mono-photon [9–11], and mono- Z/W boson [12–14] events.

In this work, we consider the singlet fermionic DM (SFDM) model mediated by an additional real scalar field, as studied in Refs. [15–17]. The scalar field mixes with the SM Higgs field, resulting in two neutral scalar bosons (h_1, h_2) in the model. The Higgs field serves as the only portal connecting SM matter to the dark sector, and such models are commonly referred to as Higgs portal models. Since the Higgs boson couples directly to the dark sector in this setup, mono-Higgs events can be a distinctive signal of the Higgs portal scenario. Moreover, the mono-Higgs production via initial state radiation is highly suppressed due to the small Yukawa couplings of light quarks. As a result, observation of these events would provide a direct probe of the interaction between the dark sector and the SM Higgs. In this context, the ATLAS and CMS collaborations have recently investigated various decay modes of the Higgs boson to search for mono-Higgs production. Among these, the decay of the Higgs boson h_1 into a $b\bar{b}$ pair has the largest branching ratio [18–23], while the decays into $\gamma\gamma$ and $\tau^-\tau^+$ provide cleaner signals [24–29].

In this SFDM model, we consider a scenario in which the DM fermion is relatively light, of order 1 GeV or below, to evade stringent constraints from direct detection experiments. The precise measurement of the relic density also places strong constraints on the DM properties. In our analysis, we find that the viable parameter space is mostly limited to the resonance region, with the mass of the additional scalar h_2 being nearly twice the DM mass. If h_2 is heavier than twice the DM mass, it predominantly decays into a DM pair, which can lead to a significant enhancement in mono-Higgs production. Furthermore, the measured total width and invisible branching ratio of the Higgs boson impose stringent constraints on the model parameter space, since the SM-like Higgs boson can have a sizable branching ratio into a pair of h_2 bosons when h_2 is sufficiently light.

The recent analyses by ATLAS [18] and CMS [24] investigated mono-Higgs production at a center-of-mass (CM) energy of 13 TeV, with integrated luminosities of 139 fb^{-1} and 35.9 fb^{-1} , respectively, and set exclusion limits on two benchmark models. We compute the mono-Higgs production cross-section of the SFDM model in the signal region defined in Refs. [18, 24], taking into account current experimental constraints on the model parameters. This paper is organized as follows. In Sec. II, we describe the model and define the relevant parameters. In Sec. III, current theoretical and experimental constraints on the model are discussed. In Sec. IV, we present the mono-Higgs production cross section and discuss the discovery potential at the LHC. Finally, in Sec. V, we summarize our conclusions.

II. THE MODEL

In this paper, we adopt a DM model consisting of a Dirac fermion field ψ and a real scalar field S , both of which are SM gauge singlets. The fermion ψ serves as the DM candidate, while the scalar S plays the role of a mediator between the dark and visible sectors. As the model has been thoroughly discussed in Refs. [15–17], we summarize only the key aspects relevant to our analysis. The dark sector Lagrangian with the renormalizable interactions is then given by

$$\mathcal{L}_{DM} = \bar{\psi}(i\cancel{\partial} - M_{\psi_0})\psi + \frac{1}{2}(\partial_\mu S)(\partial^\mu S) - g_S\bar{\psi}\psi S - V_S(S, H), \quad (1)$$

where the Higgs portal potential is

$$V_S(S, H) = \frac{1}{2}M_S^2 S^2 + \lambda_1 H^\dagger H S + \lambda_2 H^\dagger H S^2 + \frac{\lambda_3}{3!}S^3 + \frac{\lambda_4}{4!}S^4. \quad (2)$$

Note that the Higgs quadratic part $H^\dagger H$ is only the portal to the singlet sector.

After electroweak symmetry breaking, the neutral component of the SM Higgs and the singlet scalar develop nonzero vacuum expectation values (VEVs), $\langle H^0 \rangle = v_h/\sqrt{2}$ and $\langle S \rangle = v_s$, respectively. By Minimizing the full scalar potentials $V_S + V_{SM}$, where

$$V_{SM} = -\mu^2 H^\dagger H + \lambda_0 (H^\dagger H)^2, \quad (3)$$

the scalar mass parameters M_S^2 and μ^2 can be expressed in terms of the scalar VEVs as follows [30]:

$$M_S^2 = -\left(\frac{\lambda_1}{2v_s} + \lambda_2\right)v_h^2 - \left(\frac{\lambda_3}{2v_s} + \frac{\lambda_4}{6}\right)v_s^2, \quad \mu^2 = \lambda_0 v_h^2 + (\lambda_1 + \lambda_2 v_s)v_s. \quad (4)$$

The neutral scalar fields h and s defined by $H^0 = (v_h + h)/\sqrt{2}$ and $S = v_s + s$ are mixed to yield the mass matrix given by

$$\mu_h^2 = 2\lambda_0 v_h^2, \quad \mu_s^2 = -\frac{\lambda_1 v_h^2}{2v_s} + \frac{\lambda_3}{2}v_s + \frac{\lambda_4}{3}v_s^2, \quad \mu_{hs}^2 = (\lambda_1 + 2\lambda_2 v_s)v_h. \quad (5)$$

The corresponding scalar mass eigenstates h_1 and h_2 are admixtures of h and s ,

$$\begin{pmatrix} h_1 \\ h_2 \end{pmatrix} = \begin{pmatrix} \cos \theta & \sin \theta \\ -\sin \theta & \cos \theta \end{pmatrix} \begin{pmatrix} h \\ s \end{pmatrix}, \quad (6)$$

where the mixing angle θ is given by

$$\tan \theta = -\frac{\mu_h^2 - \mu_s^2 - \sqrt{(\mu_h^2 - \mu_s^2)^2 + 4\mu_{hs}^2}}{2\mu_{hs}^2}. \quad (7)$$

After the mass matrix is diagonalized, we obtain the physical masses of the two scalar bosons h_1 and h_2 as follows:

$$M_1^2 = \frac{\mu_h^2 - \mu_s^2 t_\theta^2}{1 - t_\theta^2}, \quad M_2^2 = \frac{\mu_s^2 - \mu_h^2 t_\theta^2}{1 - t_\theta^2}. \quad (8)$$

We assume that M_1 corresponds to the observed SM-like Higgs boson mass in what follows.

The model contains eight independent parameters relevant for dark matter (DM) phenomenology. The singlet fermion mass is given by $M_\psi = M_{\psi_0} + g_S v_s$, where M_{ψ_0} is a free parameter and the Yukawa coupling g_S controls the interaction strength between the Dirac fermion ψ and the singlet component of the scalar sector. We treat M_ψ as an independent parameter. The six parameters in the scalar potential, $\lambda_0, \lambda_1, \lambda_2, \lambda_3, \lambda_4$, and v_s , determine the scalar masses $M_{1,2}$, the mixing angle θ , and the self-interactions of the two physical scalars h_1 and h_2 . With the SM-like Higgs boson mass fixed at $M_1 = 125$ GeV, we are left with seven independent new physics parameters. In the next section, we apply theoretical consistency conditions and current experimental constraints to restrict the viable parameter space.

III. CONSTRAINTS

In this section, we examine the phenomenological constraints on the model from both collider experiments and dark matter (DM) observations. Due to the Higgs-portal terms in Eq. (2), the electroweak interaction of the Higgs boson can be significantly modified. Depending on their masses, the scalar states h_1 and h_2 may decay into one another. To account for the Higgs decay width constraint, we derive the cubic Higgs self-coupling coefficients c_{ijk} relevant for $h_i h_j h_k$ interactions as follows:

$$\begin{aligned} c_{111} &= 6\lambda_0 v_h c_\theta^3 + (3\lambda_1 + 6\lambda_2 v_s) c_\theta^2 s_\theta + 6\lambda_2 v_h c_\theta s_\theta^2 + (\lambda_3 + \lambda_4 v_s) s_\theta^3, \\ c_{112} &= -6\lambda_0 v_h c_\theta^2 s_\theta + 2\lambda_2 v_h (2c_\theta^2 s_\theta - s_\theta^3) + (\lambda_1 + 2\lambda_2 v_s) (c_\theta^3 - 2c_\theta s_\theta^2) + (\lambda_3 + \lambda_4 v_s) c_\theta s_\theta^2, \\ c_{122} &= 6\lambda_0 v_h c_\theta s_\theta^2 + 2\lambda_2 v_h (c_\theta^3 - 2c_\theta s_\theta^2) - (\lambda_1 + 2\lambda_2 v_s) (2c_\theta^2 s_\theta - s_\theta^3) + (\lambda_3 + \lambda_4 v_s) c_\theta^2 s_\theta, \\ c_{222} &= -6\lambda_0 v_h s_\theta^3 + (3\lambda_1 + 6\lambda_2 v_s) s_\theta^2 c_\theta - 6\lambda_2 v_h s_\theta c_\theta^2 + (\lambda_3 + \lambda_4 v_s) c_\theta^3. \end{aligned} \quad (9)$$

If $M_2 < M_1/2$, the decay $h_1 \rightarrow h_2 h_2$ is kinematically allowed via the triple coupling c_{122} . The corresponding partial width is given by

$$\Gamma(h_1 \rightarrow h_2 h_2) = \frac{|c_{122}|^2}{32\pi M_1} \left(1 - \frac{4M_2^2}{M_1^2}\right)^{1/2}, \quad (10)$$

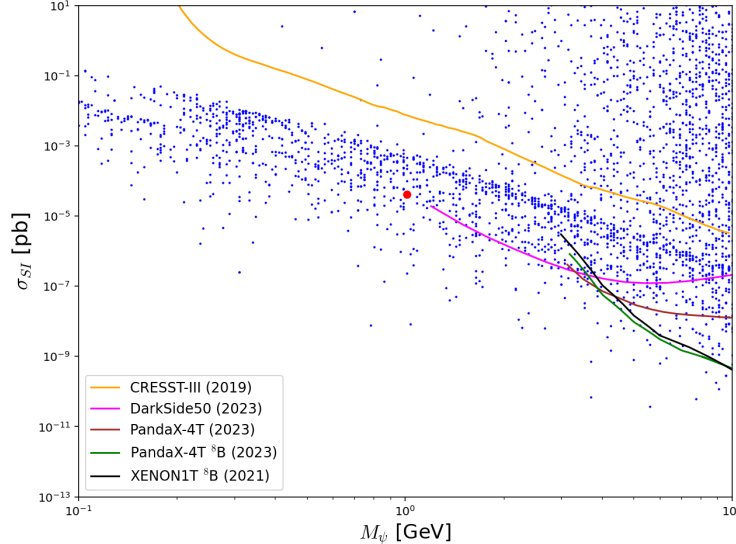


FIG. 1. Spin-independent DM-nucleon scattering cross sections allowed by relic density observations as well as the current bounds on the total Higgs decay width and its invisible branching ratio. Also shown are observed limits from CRESST-III (2019, 2022), DarkSide50 (2023), PandaX-4T (2023), XENON1T (2021), and XENONnT (2023). The red dot indicates a benchmark point chosen to discuss the mono-Higgs production analysis at the LHC.

which increases the total decay width of h_1 . Therefore, the cubic coupling c_{122} is strongly constrained by the current experimental measurement of the Higgs total decay width, $\Gamma_{\text{exp}} = 3.7^{+1.9}_{-1.4}$ MeV [31]. In addition, when $M_\psi < M_1/2$, the SM-like Higgs boson h_1 can decay directly into a pair of DM fermions via scalar mixing. The corresponding partial decay width is given by

$$\Gamma(h_1 \rightarrow \psi\bar{\psi}) = \frac{g_S^2 M_1 \sin^2 \theta}{8\pi} \left(1 - \frac{4M_\psi^2}{M_1^2}\right)^{3/2}. \quad (11)$$

Moreover, if $M_\psi < M_2/2$, the cascade process $h_1 \rightarrow h_2 h_2 \rightarrow (\psi\bar{\psi})(\psi\bar{\psi})$ also contributes to the invisible decay width of h_1 . In this case, the total invisible branching ratio of h_1 becomes

$$\text{BR}(h_1 \rightarrow \text{inv.}) = \frac{\Gamma(h_1 \rightarrow \psi\bar{\psi}) + \Gamma(h_1 \rightarrow h_2 h_2) \cdot [\text{BR}(h_2 \rightarrow \psi\bar{\psi})]^2}{\Gamma_{\text{SM}} + \Gamma(h_1 \rightarrow \psi\bar{\psi}) + \Gamma(h_1 \rightarrow h_2 h_2)}, \quad (12)$$

where $\Gamma_{\text{SM}} = 4.07$ MeV [32]. On the other hand, if h_2 decays dominantly into visible SM particles, its contribution should be excluded from the invisible branching ratio, and the numerator in Eq. (12) reduces to $\Gamma(h_1 \rightarrow \psi\bar{\psi})$. The most recent upper limit on the Higgs invisible decay branching ratio was set by the ATLAS Collaboration using 139 fb^{-1} of data at a CM energy of 13 TeV, recorded during Run 2 of the LHC [33]. They reported a combined 95% confidence-level bound of $\text{BR}(h \rightarrow \text{inv.}) < 0.107$. In applying this constraint to our model, we impose the scalar mixing angle bound $|t_\theta| \leq 0.25$, which is consistent with the LEP2 limits from the process $e^+e^- \rightarrow Zh$ for a light scalar mixed with the SM Higgs boson [34].

The precise measurement of the DM relic abundance places strong constraints on the allowed parameter space of the model. The current value of the dark matter density, $\Omega_{\text{DM}} h^2 = 0.1200 \pm 0.0012$, has been determined by global fits to cosmological observations, primarily based on the Planck satellite data, including the temperature and polarization anisotropies of the CMB, as well as its gravitational lensing measurements [35]. These precise measurements significantly limit the viable range of model parameters that can yield the correct thermal relic density. The relic density analysis in this section includes all possible channels of $\psi\bar{\psi}$ pair annihilation into the SM particles, ensuring an accurate thermal freeze-out calculation.

Using the numerical package `micrOMEGAS` [36], which employs `CalcHEP` [37] to evaluate the relevant annihilation cross sections, we compute the DM relic density and the spin-independent (SI) DM–nucleon scattering cross sections. The SI cross sections are presented in Fig. 1 as a function of the DM mass M_ψ , where the parameter points are chosen to satisfy the observed relic density as well as the current bounds on the total Higgs decay width and its invisible

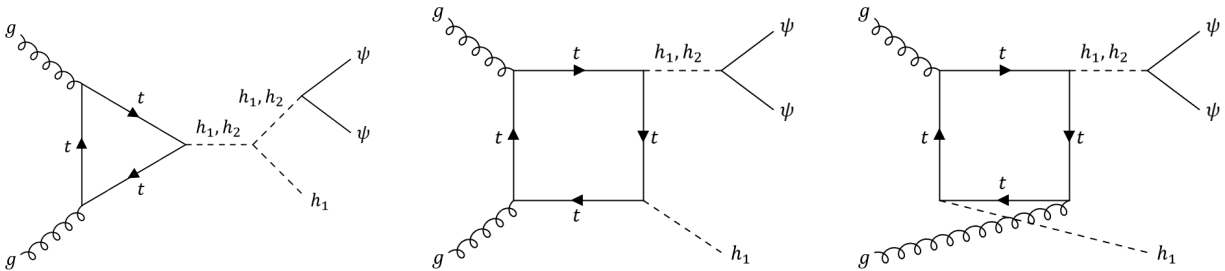


FIG. 2. Feynman diagrams for important contributions to mono-Higgs production at the LHC.

branching ratio, so that the DM sector remains consistent with Higgs precision measurements. For comparison, we overlay the 90% confidence level upper limits from CRESST-III (2019, 2022), DarkSide-50 (2023), PandaX-4T (2023), XENON1T (2021), and XENONnT (2023). Some of the recent experimental results are omitted from the figure, as their sensitivity does not reach the displayed cross-section range within the considered DM mass window.

To obtain the results shown in Fig. 1, we scan the model parameters over the following range:

$$\begin{aligned} \lambda_0 \in [0.11, 0.135], \quad \lambda_{1,3}/\text{GeV} \in [-1000, 1000], \quad \lambda_2 \in [-\pi, \pi], \quad \lambda_4 \in [0, 4\pi], \\ M_2/\text{GeV} \in [0.09, 25], \quad t_\theta \in [-0.25, 0.25], \end{aligned} \quad (13)$$

In this analysis, we also fix the new scalar VEV to $v_s = 100$ GeV and the DM Yukawa coupling to $g_S = 0.03$, which remains consistent with the constraint from the Higgs invisible decay bound for $|t_\theta| \leq 0.25$. The nonobservation of DM–nucleon scattering events is interpreted as an upper limit on the SI cross sections for a given DM mass. Figure 1 shows that the parameter sets with $M_\psi \geq 1.2$ GeV are strongly constrained by direct detection experiments. For $M_\psi < 1.2$ GeV, the DM–nucleon scattering is predominantly mediated by a t -channel exchange of the h_2 boson in most of the allowed parameter space, leading to resonance enhancements near $M_\psi \approx M_2/2$. We also highlight the red dot, which represents a benchmark point selected for the mono-Higgs production analysis at the LHC, to be discussed in the next section.

IV. SIGNATURES

The missing transverse momentum, E_T^{miss} , is defined in the experiment as the negative vector sum of the transverse momenta of all observable objects in the event, including a soft track that is matched to the primary vertex. In our theoretical analysis, E_T^{miss} arises from the production of DM fermion pairs via the decays of h_1 and h_2 . When $M_\psi > M_2/2$, the additional scalar h_2 decays only into SM particles via suppressed couplings and is generally long-lived. If the lifetime of h_2 is sufficiently long, it may escape the detector, and the process $pp \rightarrow h_1 h_2$ could mimic a mono-Higgs event. However, since the total decay width of h_2 is suppressed by $|t_\theta|^2 \sim 10^{-2}$, its lifetime is only about two orders of magnitude longer than that of the SM Higgs boson, which is not enough for h_2 to escape detection under typical collider conditions. Therefore, we do not include $pp \rightarrow h_1 h_2$ as a signal process. Instead, we consider only the process $pp \rightarrow h_1 \bar{\psi} \psi$ as the source of mono-Higgs events. The relevant Feynman diagrams for the signal process $pp \rightarrow h_1 \bar{\psi} \psi$, characterized by a Higgs boson and large missing transverse momentum in the final state, are shown in Fig. 2. In this model, the dominant contribution to the total cross section comes from gluon-gluon fusion.

The mono-Higgs production in the SFDM model is studied using a benchmark point, chosen for the purpose of analyzing the E_T^{miss} distribution, with the following numerical parameters:

$$\begin{aligned} t_\theta = 0.1958, \quad M_2 = 2.225 \text{ GeV}, \quad M_\psi = 1.012 \text{ GeV}, \quad v_s = 100 \text{ GeV}, \\ g_S = 0.03, \quad \lambda_0 = 0.128, \quad \lambda_2 = -0.3428006, \quad \lambda_4 = 8.083282, \end{aligned} \quad (14)$$

This benchmark point, indicated by the red dot in Fig. 1, is used for the cross section calculations with `MadGraph5_aMC@NLO` [38], interfaced with `Pythia8` [39] for parton showering and hadronization. Detector effects are simulated with `Delphes 3` [40], a fast simulation framework for generic collider detectors. In the `Delphes` simulation, jets are reconstructed using the anti- k_T algorithm with a radius parameter $R = 0.4$, which is consistent with typical ATLAS and CMS setups [41]. We apply basic kinematic cuts requiring jets to satisfy $p_T > 20$ GeV, rapidity $|y| < 5$ (or $|y| < 4.5$ for ATLAS), and pseudo-rapidity $|\eta| < 4.5$. Leptons are required to satisfy $|y| < 2.5$ and $|\eta| < 2.5$, and must be well separated from jets with $\Delta R(\ell, j) > 0.4$. The event generation is performed at next-to-leading order accuracy

in QCD, which ensures improved precision in modeling the hard scattering process. This simulation setup enables a reliable analysis of relevant kinematic distributions, including the missing transverse momentum, and provides predictions for potential experimental signatures of mono-Higgs events. Such signals serve as an important probe of the DM interactions with the Higgs sector, which may manifest as invisible final states at the LHC.

The normalized E_T^{miss} distribution for the process $pp \rightarrow h_1\psi\bar{\psi}$ at the CM energy of $\sqrt{s} = 13$ TeV is shown in Fig. 3. Since the DM is rather light in this model, we find that the low E_T^{miss} region is dominant in the distribution, particularly below 60 GeV. However, this region suffers from large SM backgrounds, particularly from the $Z \rightarrow \nu\bar{\nu}$ process. As a result, the ATLAS analysis in Ref. [18] imposes a requirement of $E_T^{\text{miss}} > 150$ GeV. Nevertheless, we still observe a sizable number of events in the above region.

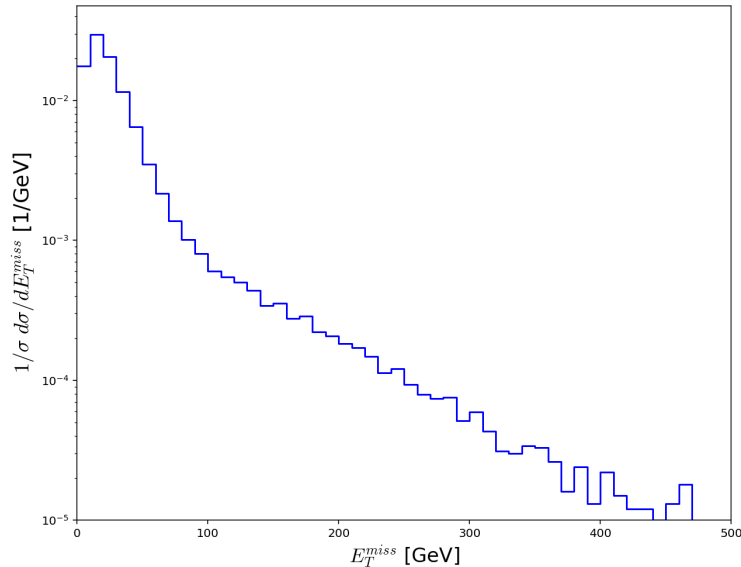


FIG. 3. E_T^{miss} distribution for $pp \rightarrow h_1\psi\bar{\psi}$ at the 13 TeV LHC for the benchmark point specified in Eq. (14).

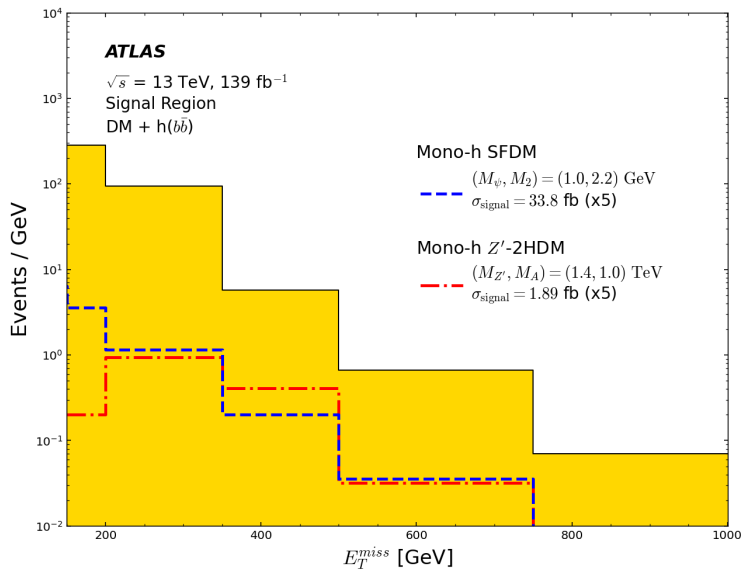


FIG. 4. Comparison of the mono-Higgs event yields predicted in the SFDM model with those from the ATLAS analysis. The estimated SFDM model prediction for the benchmark point given in Eq. (14) is shown as the blue dashed line. The event yields are shown in signal regions of E_T^{miss} , defined according to the $pp \rightarrow h_1(\rightarrow b\bar{b})X$ channel analyzed in Ref. [18]. The background expectations (shown in gold) and the benchmark model prediction (Z' -2HDM, shown as the red dash-dotted line) are taken from Fig. 6(a) of that reference.

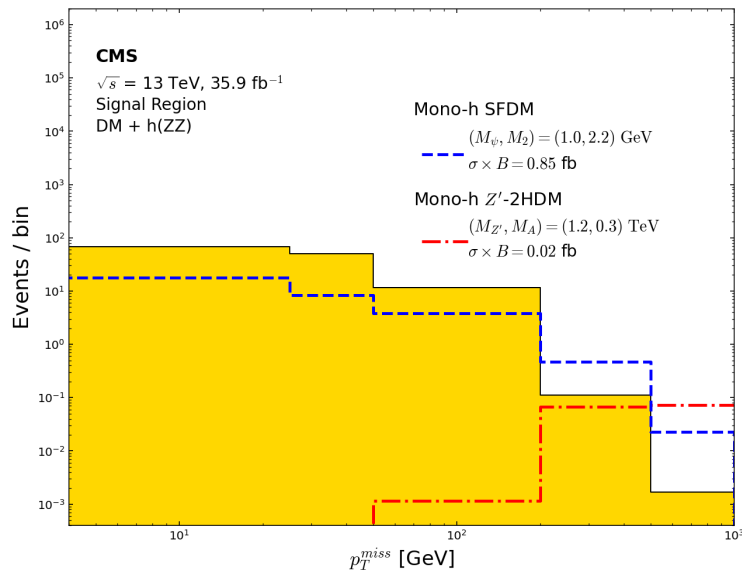


FIG. 5. Comparison of the mono-Higgs event yields predicted in the SFDM model with those from the CMS analysis. The estimated SFDM model prediction for the benchmark point given in Eq. (14) is shown as the blue dashed line. The event yields are shown in signal regions of p_T^{miss} , defined according to the $pp \rightarrow h_1(\rightarrow ZZ)X$ channel analyzed in Ref. [24]. The background expectations (shown in gold) and the benchmark model prediction (Z' -2HDM, shown as the red dash-dotted line) are taken from Fig. 6 of that reference.

We present the total yields of mono-Higgs events predicted by the SFDM model in Figs. 4 and 5. The signal regions of E_T^{miss} and the corresponding background yields follow the definitions used in the ATLAS analysis [18]. Figure 4 overlays the mono-Higgs event yields predicted in the SFDM model with those shown in Fig. 6(a) of Ref. [18], which includes ATLAS Run 2 data, SM background expectations, and a benchmark model prediction such as Z' -2HDM. We find that the SFDM model yields exceed those of the Z' -2HDM benchmark model in the $E_T^{\text{miss}} \in [150, 200)$ GeV region, and are comparable in the $[200, 350)$ GeV range. However, in the higher E_T^{miss} regions, the SFDM yields fall below those of the Z' -2HDM benchmark scenario. These results suggest that meaningful exclusion limits on the SFDM model can be derived from the non-observation of mono-Higgs events at the LHC, following the analysis strategy of Ref. [18]. Figure 5 also presents the SFDM mono-Higgs signal yields, overlaid on the expected background and benchmark prediction from the CMS $h_1 \rightarrow ZZ$ analysis [24], as shown in Fig. 6 of that reference. The Z' -2HDM benchmark curve is taken directly from the CMS result, while the SFDM prediction is superimposed for comparison. The SFDM signal prediction is substantially larger than that of the Z' -2HDM benchmark model in the relevant E_T^{miss} region, indicating a strong sensitivity to potential exclusion. As with the ATLAS case, a detailed exclusion analysis would require full detector-level simulation with CMS-specific reconstruction and selection, which is beyond the scope of this work.

V. CONCLUDING REMARKS

We have investigated the mono-Higgs production channel as a promising probe of the SFDM model at the LHC. In this model, a SM gauge-singlet Dirac fermion serves as the DM candidate, and its interactions with the visible sector are mediated by a real singlet scalar that mixes with the SM Higgs boson. This setup not only alters Higgs phenomenology but is also subject to various experimental constraints, including limits from Higgs decay properties, invisible decay bounds, relic density measurements, and direct detection experiments.

Focusing on the scenario with a relatively light DM candidate, we performed a comprehensive analysis of the mono-Higgs signature, characterized by a SM-like Higgs boson in association with large missing transverse momentum. We simulated the signal process $pp \rightarrow h_1\psi\bar{\psi}$ at $\sqrt{s} = 13$ TeV, incorporating theoretical and experimental constraints on the parameter space. A benchmark point consistent with the observed relic abundance and current Higgs bounds was selected, and the resulting E_T^{miss} distributions were studied in detail.

We compared the predicted event yields with recent results from ATLAS and CMS mono-Higgs analyses. For certain parameter choices, we found that the SFDM model yields are comparable to or even exceed those of benchmark models

like Z' -2HDM in the low-to-intermediate $E_{\text{T}}^{\text{miss}}$ regions. These results suggest that the SFDM model can be effectively tested by ongoing LHC searches for mono-Higgs events.

The High Luminosity LHC (HL-LHC) is anticipated to substantially improve the sensitivity to mono-Higgs signatures. Based on our analysis, future data may enable meaningful exclusion or potential discovery of the viable SFDM parameter space, offering a complementary pathway to probe Higgs-portal DM scenarios.

ACKNOWLEDGMENTS

This work is supported by Basic Science Research Program through the National Research Foundation of Korea (NRF) funded by the Ministry of Education under the Grant No. RS-2023-00248860 (S.-h.N.) and also funded by the Ministry of Science and ICT under the Grants No. NRF-2021R1A2C2011003 (K.Y.L.).

-
- [1] G. Bertone and D. Hooper, *Rev. Mod. Phys.* **90**, no.4, 045002 (2018).
 - [2] M. Bauer and T. Plehn, *Lect. Notes Phys.*, Vol. **959** (Springer, 2019).
 - [3] Y. Mambrini, Springer, 2021, ISBN 978-3-030-78138-5, 978-3-030-78139-2.
 - [4] D. J. E. Marsh, D. Ellis and V. M. Mehta, Princeton University Press, 2024, ISBN 978-0-691-24971-1, 978-0-691-24952-0.
 - [5] M. Cirelli, A. Strumia and J. Zupan, arXiv:2406.01705 [hep-ph].
 - [6] G. Aad *et al.* [ATLAS], *Phys. Rev. D* **103**, no.11, 112006 (2021).
 - [7] A. M. Sirunyan *et al.* [CMS], *Phys. Rev. D* **97**, no.9, 092005 (2018).
 - [8] T. Aaltonen *et al.* [CDF], *Phys. Rev. Lett.* **108**, 211804 (2012).
 - [9] G. Aad *et al.* [ATLAS], *JHEP* **02**, 226 (2021).
 - [10] A. M. Sirunyan *et al.* [CMS], *JHEP* **10**, 073 (2017).
 - [11] T. Aaltonen *et al.* [CDF], *Phys. Rev. Lett.* **101**, 181602 (2008).
 - [12] M. Aaboud *et al.* [ATLAS], *JHEP* **10**, 180 (2018).
 - [13] A. M. Sirunyan *et al.* [CMS], *JHEP* **07**, 014 (2017).
 - [14] M. Aaboud *et al.* [ATLAS], *Phys. Lett. B* **776**, 318-337 (2018).
 - [15] Y. G. Kim and K. Y. Lee, *Phys. Rev. D* **75**, 115012 (2007).
 - [16] Y. G. Kim, K. Y. Lee and S. Shin, *JHEP* **05**, 100 (2008).
 - [17] Y. G. Kim, K. Y. Lee, C. B. Park and S. Shin, *Phys. Rev. D* **93**, no.7, 075023 (2016).
 - [18] G. Aad *et al.* [ATLAS], *JHEP* **11**, 209 (2021).
 - [19] M. Aaboud *et al.* [ATLAS], *Phys. Rev. Lett.* **119**, no.18, 181804 (2017).
 - [20] M. Aaboud *et al.* [ATLAS], *Phys. Lett. B* **765**, 11-31 (2017).
 - [21] G. Aad *et al.* [ATLAS], *Phys. Rev. D* **93**, no.7, 072007 (2016).
 - [22] A. M. Sirunyan *et al.* [CMS], *Eur. Phys. J. C* **79**, no.3, 280 (2019).
 - [23] A. M. Sirunyan *et al.* [CMS], *JHEP* **10**, 180 (2017).
 - [24] A. M. Sirunyan *et al.* [CMS], *JHEP* **03**, 025 (2020).
 - [25] G. Aad *et al.* [ATLAS], *JHEP* **10**, 013 (2021).
 - [26] M. Aaboud *et al.* [ATLAS], *Phys. Rev. D* **96**, no.11, 112004 (2017).
 - [27] G. Aad *et al.* [ATLAS], *Phys. Rev. Lett.* **115**, no.13, 131801 (2015).
 - [28] A. M. Sirunyan *et al.* [CMS], *JHEP* **09**, 046 (2018).
 - [29] G. Aad *et al.* [ATLAS], *JHEP* **09**, 189 (2023).
 - [30] S. Profumo, M.J. Ramsey-Musolf and G. Shaughnessy, *J. High Energy Phys.* **0708**, 010 (2007).
 - [31] S. Navas *et al.* [Particle Data Group], *Phys. Rev. D* **110**, no.3, 030001 (2024).
 - [32] D. de Florian *et al.* [LHC Higgs Cross Section Working Group], arXiv:1610.07922 [hep-ph].
 - [33] G. Aad *et al.* [ATLAS], *Phys. Lett. B* **842**, 137963 (2023).
 - [34] R. Barate *et al.* [LEP Working Group for Higgs boson searches, ALEPH, DELPHI, L3 and OPAL], *Phys. Lett. B* **565**, 61-75 (2003).
 - [35] N. Aghanim *et al.* [Planck], *Astron. Astrophys.* **641**, A6 (2020); erratum: *Astron. Astrophys.* **652**, C4 (2021).
 - [36] G. Bélanger, F. Boudjema, A. Goudelis, A. Pukhov and B. Zaldivar, *Comput. Phys. Commun.* **231**, 173-186 (2018).
 - [37] A. Belyaev, N. D. Christensen and A. Pukhov, *Comput. Phys. Commun.* **184**, 1729-1769 (2013).
 - [38] J. Alwall *et al.*, *JHEP* **07**, 079 (2014).
 - [39] T. Sjöstrand *et al.*, *Comput. Phys. Commun.* **191**, 159-177 (2015).
 - [40] J. de Favereau *et al.* [DELPHES 3], *JHEP* **02**, 057 (2014).
 - [41] N. Anjos [ATLAS and CMS], *EPJ Web Conf.* **120**, 05005 (2016).